

Residual Stresses in Layered Manufacturing

A. Nickel, D. Barnett, G. Link, and F. Prinz

Department of Materials Science and Engineering, Stanford University

Abstract

Layered Manufacturing processes accumulate residual stresses during material build-up. These stresses may cause part warping and layer delamination. This paper presents work done on investigating residual stress accumulation and part distortion of Layered Manufactured artifacts. A simple analytical model was developed and used to determine how the number of layers and the layer thickness influences part warping. Results show that thin layers produce lower part deflection as compared with depositing fewer and thicker layers. In addition to the analytical work, a finite element model was developed and used to investigate the deposition pattern's influence on the part deflection. Finite element model and corresponding experimental analysis showed that the geometry of the deposition pattern significantly affects the resulting part distortion. This finite element model was also used to investigate an inter-layer surface defect, known as the Christmas Tree Step, that is associated with Shape Deposition Manufacturing. Results indicate that the features of this defect are influenced only by the material deposited close to the part surface and the particular material deposited. The step is not affected by the deposition pattern.

1 Introduction

Residual stresses develop in many Layered Manufacturing processes. These stresses arise from the contraction or expansion associated with the deposition of a layer, which causes distortions and possibly failure by layer delamination or cracking. Many authors have examined residual stresses in Layered Manufacturing. Jayanthi et al. [1], Ullett et al. [2], and Jacobs [3] each discuss how the scanning pattern of the laser in Stereolithography affects the resulting deflection of the part, while Karapatis et al. [4] and Dalgarno et al. [5] studied residual stresses in metal parts produced using Selective Laser Sintering. McIntosh et al. [6] examined deformation of ceramic parts produced using Fused Deposition of Ceramics. Both Maziasz et al. [7] and Griffith et al. [8] measured residual strain in H13 tool steel parts produced by Laser Engineered Net Shaping. In addition, Chin et al. [9,10] and Klingbeil et al. [11,12] examined residual stresses and deformation in microcasted metal parts produced using Shape Deposition Manufacturing (SDM). In all of these processes residual stresses accumulate and lower the quality of the manufactured parts.

This research focused on thermal stresses in laser deposited metal parts produced using SDM. SDM is a Layered Manufacturing process developed jointly at Carnegie Mellon University and Stanford University [13]. SDM's unique features include material removal after each layer is deposited and the use of a sacrificial support material to facilitate the deposition of overhanging structures. Metal parts are produced by feeding powders into a molten pool formed by a 2.4 KW Nd:YAG laser. The laser and the powder feed are then scanned over the surface of the part producing a deposited layer. After several laser passes, the desired layer thickness is achieved and the excess material is then removed with a computer controlled (CNC) milling machine. Thermal stresses in these parts were investigated using a combination of analytical modeling, finite element modeling, and experiments. Initially an analytical model was developed to predict the overall part warpage. Then both a finite element model and experiments were used to investigate how the pattern used to deposit a layer influences the substrate warpage, and to investigate the inter-layer surface defect known as the Christmas Tree Step.

2 Analytical Model

This research began by first developing an analytical model to predict substrate warpage. Both elastic and elastic-perfectly plastic models were investigated. These models are similar to the models developed by Townsend et al. [14]. In this model, the radius of curvature of the substrate, or equivalently, the substrate deflection was determined (figure 1). To solve for the deflection, the time dependent laser deposition process was approximated with two time steps. The first step includes the laser heating, and the second step includes the beam cooling after the laser energy is removed. The conditions of equilibrium, namely the summation of the forces to zero and the summation of the moments to zero were then used to determine the deflection. In the elastic-perfectly plastic model, additional continuity conditions were necessary to solve for the position of the elastic plastic boundaries.

The results of the calculation for a 6.3 mm x 25.4 mm x 152.4 mm beam substrate are shown in table 1. In addition, experiments were performed for comparison with the calculated results. The experimental values are shown in table 2. The elastic analytical

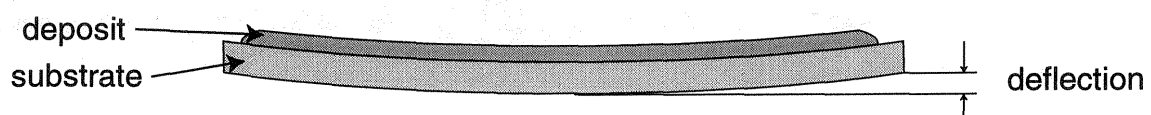


Figure 1: Deflection of a beam substrate subjected to laser deposition.

Model	Bolting Conditions	1/R	Deflection Invar 36	Deflection 1117 steel
Elastic	no constraint	$\frac{3}{4h} \alpha (T_{room} - T_{melt}) (1 - (\frac{r}{h})^2)$	0.82 mm	6.21 mm
Elastic-Perfectly Plastic	no constraint	$-12 \frac{\sigma_{yield}}{E} \frac{h(h-r)}{(r+h)^3}$	not valid	0.83 mm
	constrain bending	$-\frac{3}{2} \frac{\sigma_{yield}}{E} \frac{(h-r)}{h^2}$	not valid	0.50 mm
	constrain bending and axial	$-\frac{3}{4} \frac{\sigma_{yield}}{E} \frac{(h^2-r^2)}{h^3}$	not valid	0.16 mm

Table 1: Calculated deflection values for 6.3 mm x 25.4 mm x 152.4 mm (1/4 in x 1 in x 6 in) substrates where $2h$ is the thickness of the substrate, α is the expansion coefficient, T_{room} is room temperature, T_{melt} is the melting temperature, $(h - r)$ is the depth of remelting, σ_{yield} is the yield strength, and E is the elastic modulus.

model accurately predicted the deflection for Invar substrates. However, the elastic-perfectly plastic model was necessary for low carbon steel substrates due to the significant amount of plastic deformation that occurs in these substrates. As shown in table 1 the elastic-perfectly plastic equations are not valid for Invar since no plasticity occurs in the calculation for Invar substrates. The results show that for the elastic-perfectly plastic model, bolting the substrate down during deposition reduced the part deflection. Chin et. al. [9] noted a similar result for microcasted SDM metal parts. The results of this calculation also show the deflection dependence on material and process properties. In the elastic model the deflection depends on the expansion coefficient, the remelted depth, and the change in temperature that occurs during the substrate cooling. In the elastic-perfectly plastic model the deflection depends on the yield strength, the elastic modulus, and the remelted depth. Table 2 shows that the experimental deflection depends on the deposition pattern. The deflection dependence on the deposition pattern cannot be modeled analytically and is discussed using a finite element model in the next section.

Pattern	Bolting Condition	Deflection Invar 36	Deflection 1117 steel
long raster	bolted	0.79 mm	1.00 mm
short raster	bolted		0.44 mm

Table 2: Experimental deflection values for 6.3 mm x 25.4 mm x 152.4 mm (1/4 in x 1 in x 6 in) substrates

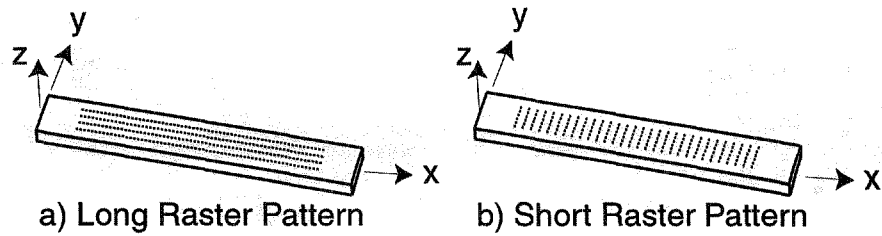


Figure 2: Long and short raster deposition patterns for a beam substrate.

This model was then used to examine how the deposit thickness and the number of layers used to produce the deposit influences the warpage of the part. The deflection of a beam substrate is plotted against the deposit thickness in figure 3. Each line in this graph represents a constant number of layers used to achieve the desired deposit thickness. The results indicate that depositing thinner layers reduces the deflection and that the majority of the deflection accumulates for deposit thicknesses up to the substrate thickness.

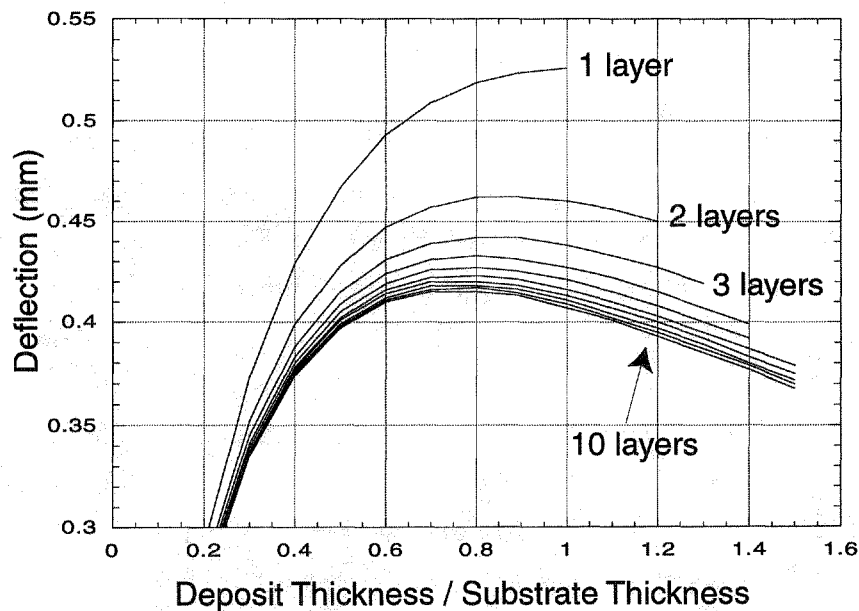


Figure 3: Deflection verses deposition thickness and the number of layers used to produce the deposition.

3 Deposition Pattern

In SDM of metal parts many deposition patterns can be used to deposit a layer. The pattern used has a significant influence on the substrate warpage. The deflection depen-

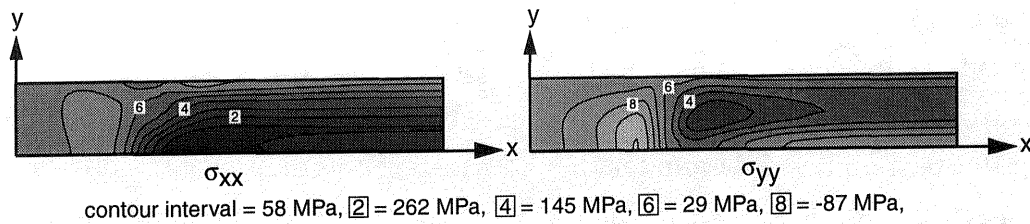


Figure 4: The finite element calculated stresses on the top surface of a beam substrate after the last line in the long raster pattern has been scanned and the substrate has cooled to room temperature.

dence on the deposition pattern was investigated using both finite element modeling and experiments.

The finite element results for a 6.3 mm x 25.4 mm x 152.4 mm beam substrate are shown in figures 4 and 5. In figure 4 the final σ_{xx} and σ_{yy} stresses on the top surface of a beam substrate is shown due to a long raster deposition pattern (figure 2). Only 1/4 of the beam is shown due to assumed symmetry planes along the x and y axis. This figure shows that the highest stresses are found along the deposition lines. Since the deposition lines are oriented in the x direction for the long raster pattern, the σ_{xx} stress is larger than the σ_{yy} stress as shown in figure 4. Similar results were reported by Andersson [15] and Jonsson et al. [16] for stresses in welded structures. In figure 5 the σ_{yy} stress is shown after the first line in the short raster pattern has cooled and after the last line in the short raster pattern has cooled. This figure shows that the highest stresses are found where the last line was deposited.

The optimal deposition patterns for both a 6.3 mm x 25.4 mm x 152.4 mm beam and a 6.3 mm x 152.4 mm x 152.4 mm plate substrates were determined from these observations. The lowest deflection for a beam substrate occurs by minimizing the σ_{xx} stress. Since the short raster pattern does not have any deposition lines oriented along the x axis, it produces

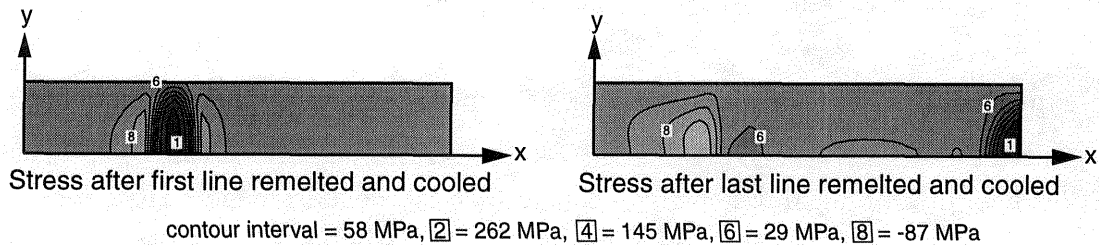


Figure 5: The finite element-calculated σ_{yy} stress at the top surface of a beam substrate after the first line and the last line in the short raster pattern has been scanned and the substrate has cooled to room temperature.

the lowest σ_{xx} stress. Therefore, this pattern results in the lowest beam deflection. The finite element calculated deflection values were 0.92 mm for the long raster pattern and 0.39 mm for the short raster pattern. These results match closely the experimental values of 1.00 mm for the long raster pattern and 0.44 mm for the short raster pattern. Using the observation that the highest stresses are found where the last line was deposited, the lowest deflection for a plate substrate occurs by minimizing the length of the last line deposited. Therefore, a spiral pattern scanned from the outside to the inside will produce low and uniform stresses for a plate substrate. The finite element-calculated value for the deflection along the centerline of the plate was 0.34 mm and the experimental value was 0.49 mm. This deflection is contrasted with a spiral pattern scanned in the opposite direction which has a calculated deflection of 0.55 mm and an experimental deflection of 0.60 mm. Klingbeil et al. [12] experimentally observed similar deflections for microcast patterns on plate substrates.

4 Christmas Tree Step

SDM suffers not only from the global distortion previously discussed, but also from a local defect known as the Christmas Tree Step. This step is found at the layer interface and results in poor surface quality and part inaccuracy. Figure 6 shows this defect on a metal part.

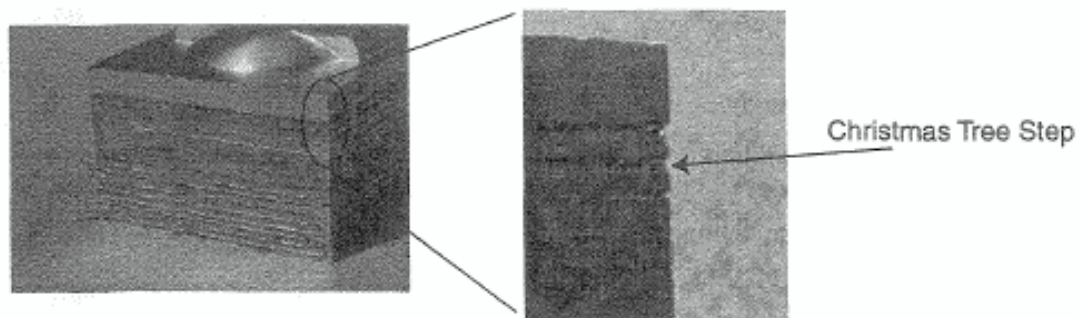


Figure 6: The Christmas Tree Step on a metal part.

An experiment was performed to investigate which processing steps influence the magnitude of the Christmas Tree Step. The experiments showed that the support material deposition and machining did not significantly distort the part edge. However, if sharp cutters and small cutting depths were not used, removal of excess support material could significantly deform the edge of the part. The experiments also show that the majority of this distortion develops during the deposition of the part material.

A finite element model and experiments were used to make three observations on the

development of the Christmas Tree Step. Firstly, it was determined that the step is an edge effect. Figure 7 shows the step size as a function of the deposition length for a 0.75 mm thick deposited layer. Both the finite element and experimental results in this figure show that the step develops due to the material deposited close to the edge of the part. Secondly, it was determined that the step size does not depend significantly on the deposition pattern. Experimentally the average step size for a 0.75 mm thick layer deposited using a long raster deposition was 46.9 μm , and the step size obtained using a short raster pattern was 39.6 μm . These results show that there is only a small difference in step size for the two different deposition patterns. Finally, experimentally the step size was found to depend on the particular material deposited. The step size for a 3 mm thick was 102 μm , 70 μm , and 33 μm for 316 stainless steel, Invar, and 410 stainless steel, respectively. It is believed that this martensitic 410 stainless steel produced the lowest step size due to the solid state phase transformations that occur upon cooling and on subsequent reheating during future depositions.

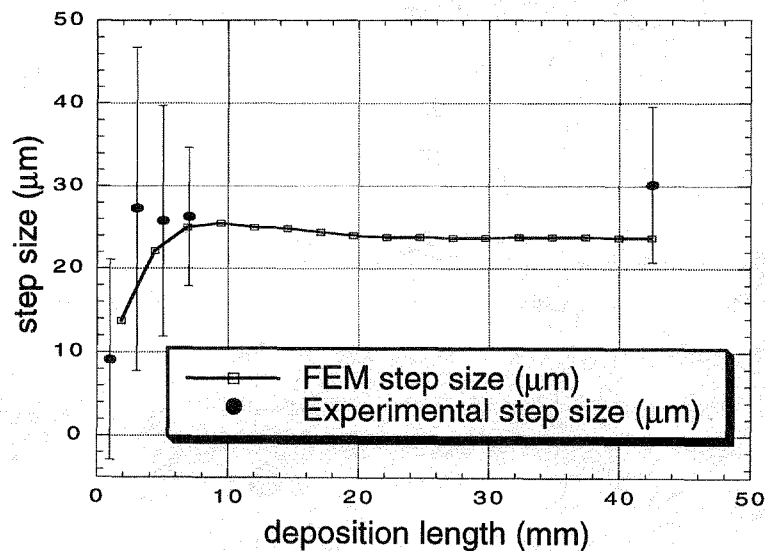


Figure 7: The Christmas Tree Step size as a function of deposition length.

5 Conclusion

This research increased the understanding of residual stress accumulation in metal parts produced using Shape Deposition Manufacturing. The combination of analytical modeling, finite element modeling and experiments was used to predict overall part deflection, to understand the influence of deposition patterns on part warpage, and to understand the

development of the Christmas Tree Step. Although these results were found while researching metal parts produced using SDM, many of the findings are applicable to parts produced using other Layered Manufacturing processes. The elastic-perfectly plastic model results are applicable to any Layered Manufacturing processes that involve some form of permanent deformation during cooling. Also, the deposition pattern findings are valid for processes that produce layers by scanning material over the part surface. In addition, the results from the Christmas Tree Step analysis give insight into the local deformation processes that occur near the part edges for many Layered Manufacturing techniques. To produce accurate Layered Manufactured parts, continuing research is necessary to understand and reduce the adverse affects of residual stress accumulation.

6 Acknowledgments

The authors gratefully acknowledge the Department of the Army for administrating contract #DAAH04-96-1-0241 for the Defense Advance Research Projects Agency and the Office of Naval Research (#N00014-96-1-0354) for their support of this research.

7 References

- [1] S. Jayanthi et al., Proc. Solid Freeform Fabrication Sym., 250-258, 1997.
- [2] J. Ullett et al., Proc. Solid Freeform Fabrication Sym., 242-249, 1994.
- [3] P. Jacobs, Rapid Prototyping and Manufacturing, 1996.
- [4] N. Karapatis et al., Proc. Solid Freeform Fabrication Sym., 79-87, 1998.
- [5] K. Dalgarno et al., Proc. Solid Freeform Fabrication Sym., 721-728, 1998.
- [6] J. McIntosh et al., Proc. of the Solid Freeform Fabrication Sym., 159-166, 1997.
- [7] P. Maziasz et al., Scripta Materialia, 39(10):1471-1476, 1998.
- [8] M. Griffith et al., Proc. Solid Freeform Fabrication Sym., 89-96, 1998.
- [9] R. Chin et al., Proc. Solid Freeform Fabrication Sym., 221-228, 1995.
- [10] R. Chin et al., Proc. Solid Freeform Fabrication Sym., 507-514, 1996.
- [11] N. Klingbeil et al., Proc. Solid Freeform Fabrication Sym., 125-132, 1997.
- [12] N. Klingbeil et al., Proc. Solid Freeform Fabrication Sym., 367-374, 1998.
- [13] R. Merz et al., Proc. Solid Freeform Fabrication Sym., 1-8, 1996.
- [14] P. Townsend et al., J. Applied Physics, 62(11):4438-4444, 1987.
- [15] B. Andersson, J. Eng. Mat. Tech., 100(4):356-362, 1978.
- [16] M. Jonsson et al., Numerical Methods in Heat Transfer, vol. 3, chap. 2, 1985.